THE SOCIETY OF NAVAL ARCHITECTS AND MARINE ENGINEERS
One World Trade Center, Suite 1369, New York, N.Y. 10048

Papers to be presented at Extreme Loads Response Symposium
Arlington, VA, October 19–20, 1981

# Evaluation of Ultimate Ship Hull Strength

**R. S. Dow, R. C. Hugill, J. D. Clark** and **C. S. Smith,**
Admiralty Marine Technology Establishment, Glasgow, Scotland

ABSTRACT

The problem of evaluating the ultimate longitudinal strength of a ship's hull is discussed. In addition to behaviour under quasi-static loads, the whipping response of a ship's hull to impulsive loads, eg bow-slamming and underwater explosions, is considered. A method of analysis is described, based on approximate characterization of the strength of elements of hull cross-sections under tensile and compressive loads associated with hull-girder bending together with local lateral-pressure effects. The influence of imperfections (initial deformations and residual stresses) is accounted for. The analysis is illustrated with reference to a typical warship hull design. Theoretical results are correlated with experimental data derived from collapse tests on a number of stiffened box-girders.

## INTRODUCTION

Assessment of the ultimate longitudinal strength of a ship's hull under loads imposed by the sea has traditionally been made by comparing calculated elastic stresses in the deck or bottom shell with allowable stresses, usually corresponding to prescribed fractions of the material yield strength. This approach, applied in conjunction with a nominal estimate of vertical wave bending moment based on static-balance analysis, has a certain empirical validity when applied to conventional ships closely resembling previous successful hulls designed in the same way, but fails to provide a true estimate of hull strength and is clearly unsatisfactory when applied to unconventional designs. If the hull structure does not fail locally, the actual collapse bending moment may exceed the moment which nominally causes outer-fibre yield; on the other hand the collapse moment may be substantially less than the nominal yield moment if local compressive failure of plating or stiffened panels occurs in parts of the cross-section.

A recent trend in the design of ships, offshore platforms and civil engineering structures is towards use of limit-state design criteria, requiring explicit consideration of ultimate strength in relation to statistically defined loads. Some effort has consequently been devoted to evaluation of ultimate, elasto-plastic strength of ships' hulls (1 to 6)* and a method of estimating hull strength has been proposed (4) which takes account of local buckling failure and post-collapse loss of load-carrying capacity in elements of the hull cross-section. The purpose of the present paper is to examine the accuracy of this approach by correlation of analysis with collapse tests on various longitudinally stiffened steel box-girders and to consider extension of the analysis method to deal with the case of dynamic loading, in particular whipping of the hull girder caused by bow-slamming or underwater explosions which, as shown by recent theoretical studies and seakeeping trials, may cause severe midship bending moments.

## STATIC ANALYSIS OF HULL STRENGTH

### Strength and Stiffness of Plate Elements

Between 60% and 80% of a typical hull cross-section is formed by deck, shell and longitudinal bulkhead plating: hull strength is therefore likely to be critically influenced by the stiffness and strength of plate elements, particularly under compressive load. Loss of stiffness in the plating, which may be caused by buckling or premature yielding, leads directly to loss of effective moment of inertia and section modulus in a hull cross-section and also accelerates yield in the stiffeners and hence elasto-plastic buckling of stiffened panels.

In longitudinally framed deck and shell structure containing closely spaced stringers with relatively widely spaced transverse frames, plates of aspect ratio a/b (length/breadth) > 1.5 will buckle into one or more half-waves of length $\lambda$ somewhat less than the plate breadth ($0.7 < \lambda/b < 1.0$). Various approximate methods of characterizing the strength and stiffness of such plates, based on large-deflection elastic analysis or on interpretation of test data, have been reviewed by Faulkner (7). A much improved understanding of plate buckling has been obtained in recent years from the application of nonlinear finite element and finite difference analysis representing large deflection elasto-plastic behaviour (8 to 13): parametric application of such analysis, accounting for imperfections (distortions and residual stresses) as

* Denotes references at end of paper.

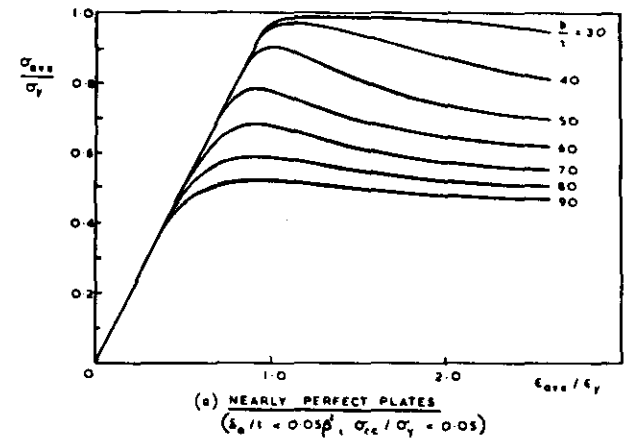


Fig. 1 Load-Shortening Curves for Square Plates under Uniaxial Compression $\left(\beta = \frac{b}{t}\sqrt{\frac{\sigma_y}{E}}\right)$

measured in surveys of ships and welded steel box-girder bridges (13, 14) has led to data curves of the type shown in Figure 1 (13) which have the merit of defining not only maximum load-carrying capacity but also plate stiffness at any point in the strain range. The curves shown in Figure 1 have been derived from analysis of simply supported square or nearly square plates with longitudinal edges constrained to remain straight but free to move bodily in the plane of the plating. Over the strain range preceding plate failure these curves may be applied without modification to long rectangular plates on the assumption that buckling occurs in approximately square half-waves and that compressive strain occurs uniformly over the full length of each plate: in the post-collapse range, where end-shortening strain may be confined to a single, approximately square collapse zone with virtually zero increase of strain over the remainder of the plate, a simple correction dependent on the aspect ratio a/b may be applied to the strain scale.

In the case of transversely framed deck and shell structure, as commonly employed in the fore and after regions of a ship's hull, failure of wide plate panels (a/b << 1) under longitudinal compression is likely to occur by buckling into single lobes over the full width of each plate. Recent numerical studies (15, 16, 17) have provided some information about the stiffness, strength and imperfection sensitivity of such plating. It has been shown that loss of stiffness and strength depends critically on the form of initial deformation, as shown in Figure 2. Some strength curves for very wide plates (b/a → ∞) having initial deformations of symmetric and antisymmetric form (17), together with curves derived from References 15 and 16 for wide plates of finite aspect ratio ($1 \leq b/a \leq 5$) having various levels of antisymmetric distortion, are shown in Figure 3.

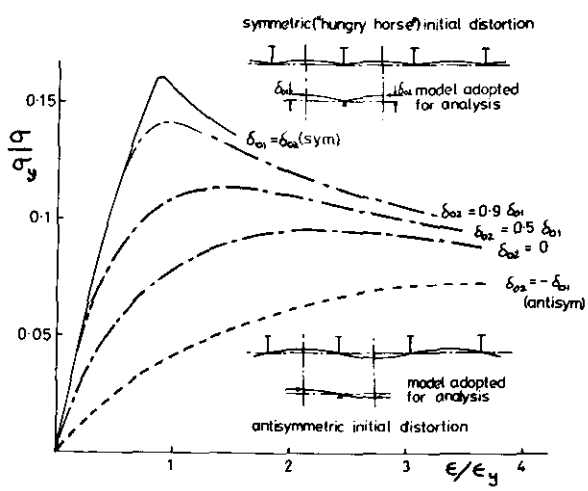


Fig. 2 Load-Shortening Curves for Transversely Compressed Long Plates (a/b = ∞) with Symmetric, Antisymmetric and Intermediate Forms of Distortion

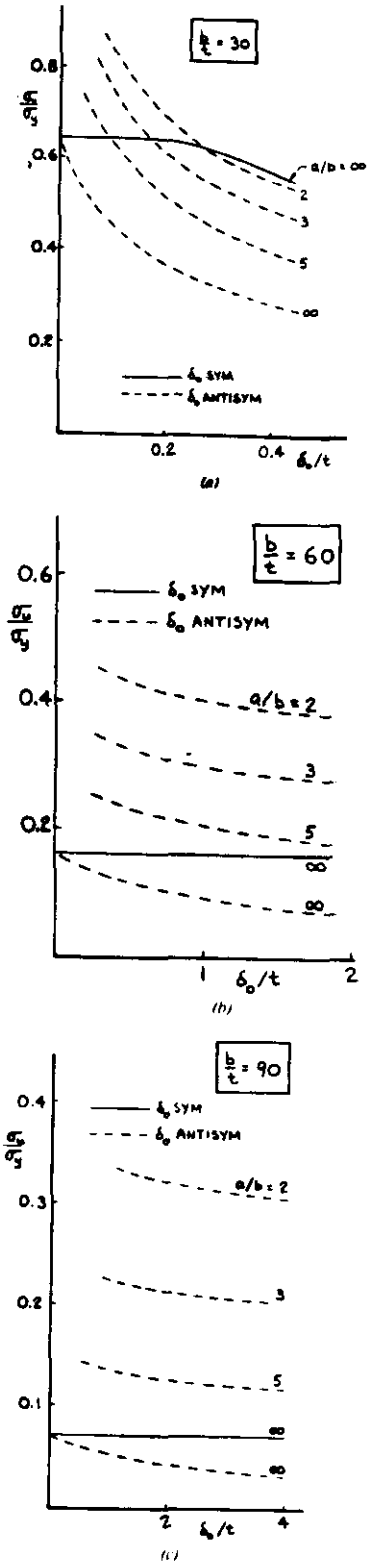


Fig. 3 Strength Curves for Wide Plates Under Compression in Shorter Direction

## Strength and Stiffness of Stiffened Panels

It has been shown (18) that the most likely form of failure in flat panels of orthogonally stiffened plating forming bottom shell and deck structures in ships is column-like interframe flexural buckling of longitudinal stiffeners with attached plating under longitudinal compression induced by hull bending: this form of failure, which may be strongly influenced by loss of compressive stiffness of the plating, will in most practical cases precede other collapse modes including lateral-torsional buckling of girders and overall buckling involving bending of transverse frames.

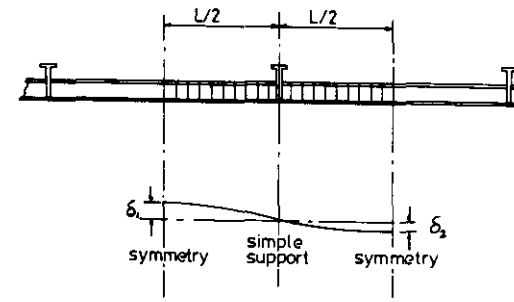


a) Subdivision of stiffened panel into elements showing assumed initial deformation

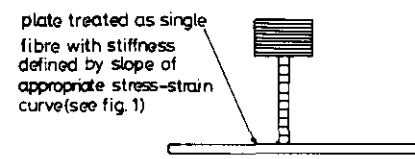


b) Subdivision of cross section into fibres

Fig. 4 Idealisation of Stiffened Panels

For the purpose of examining the column-like interframe flexural buckling of closely spaced longitudinal stiffeners with attached plating under longitudinal compression, analysis may be confined to a single stiffener with attached strip of plating treated as a beam column with conditions of simple or elastic support at positions of transverse frames as shown in Figure 4a. In order to examine the large deflection, inelastic buckling behaviour of such structures, a computer program has been developed (18, 19) for the nonlinear analysis of plane frames of general geometry, including straight or initially deformed beam columns as a special case. The main features of the analysis method are as follows:

(i) Frames of arbitrary polygonal or curved geometry are represented as assemblies of straight beam elements. Polygonal representation of curved

frames will give satisfactory results provided that a sufficient number of straight line elements are included in the idealisation. In accordance with normal beam theory the element employed has a cubic representation of flexural deformation (w) and a linear representation of extensional deformation (u). Full account is taken of the coupled flexural and extensional deformations of a frame. Plane sections are assumed to remain plane under conditions of elastic and inelastic bending and extension.

Provision is made for finite separation between node points at the ends of elements, account thus being taken of changes in the position of the element elastic neutral axes (caused by progressive yielding or local buckling of cross sections) and consequent eccentricity of element axial forces.

(ii) Initial deformations may have any form, being defined for analysis purposes as part of the initial structural geometry.

(iii) Sectional properties are assumed to be constant in each element but may vary from one element to another. Cross sections are divided into elemental areas corresponding to frame "fibres" (Figure 4b); residual stresses, which may have any distribution over a frame section, are represented as initial stresses at fibre centroidal positions.

(iv) The method of analysis employed is the linearised incremental finite element process, in which loads (or displacements) are applied incrementally, a linear solution being obtained for each incremental load application by the usual matrix displacement method, ie by solving the incremental matrix equation:

$$\left[K_T\right] \{\Delta\delta\} = \{\Delta P\} \qquad (1)$$

where $K_T$ - is the tangent stiffness matrix ($K_T = K_E + K_G$)

$K_E$ - is the conventional elastic stiffness matrix representing the axial and flexural stiffness of frame elements

$K_G$ - is the geometric stiffness matrix representing the destabilising influence of axial forces in frame elements

$\Delta\delta$ - is the column vector of incremental nodal displacements

$\Delta P$ - is the column vector of incremental nodal loads

The above linearised incremental process is coupled with a generalised Newton Raphson iterative equilibrium correction scheme based on the matrix equation:

$$\{\delta\}_{j+1} = \{\delta\}_j + \left[K_T\right]_j^{-1} \left(\{P_{ext}\} - \{P_{int}\}\right) \qquad (2)$$

The expression in parenthesis represents the unbalanced forces arising from the application of the linearised incremental procedure. The gradient for the iterations is updated for every iteration cycle. The vector $\{P_{ext}\}$ is the total applied load vector and $\{P_{int}\}$ is the total internal load vector calculated from integration of the total fibre stresses. The equilibrium iterations are terminated when the unbalanced forces have converged to a specified percentage of the total applied loads.

(v) Following each incremental solution, cumulative values of nodal displacements, together with stresses, strains and destabilising forces in the frame elements, are updated. The state of stress of each fibre of each element is examined and where the total average stress (including initial residual stress) in the fibre exceeds the yield stress, the fibre is taken either

(a) to contribute no stiffness in the next incremental step, an elastic-perfectly plastic material stress-strain curve being assumed, or

(b) to have a reduced modulus derived from a numerically defined stress-strain curve of any prescribed shape.

Option (a) has been adopted for steel structures defined in the present paper. The element elastic section properties, element stiffness coefficients and hence the stiffness matrix for the complete frame are modified accordingly before entering the next incremental solution.

(vi) Allowance is made for elastic unloading of yielded fibres: ie where elastic unloading is found to have

occurred in a yielded fibre following an incremental cycle, the fibre is assumed to recover its elastic section properties for the next incremental step.

(vii) Where part of a frame cross-section is formed by a strip of slender plating it may be necessary to allow for loss of stiffness caused by local plate buckling: provision has been made in the analysis for treatment of the plate as a single fibre whose incremental stiffness is derived as a function of average compressive strain from the slopes of the load-shortening curves shown in Figure 1.

(viii) The effect of large deflections is allowed for by updating the element co-ordinate system and structural geometry, following each incremental cycle (Updated Lagrangian Formulation). This approach allows the post collapse behaviour of certain structures to be examined, including particularly that of beam columns under prescribed end shortening.

(ix) Load application is normally divided into several ranges, large increments being taken in the first range where the behaviour is elastic reducing progressively to small increments as the collapse load is approached. A restart facility has been built into the program: this enables the user to change the solution strategy and increment size as the calculation progresses, thus making the solution process more efficient especially for large problems where little information about the nonlinear behaviour is known in advance.

Hull-Girder Strength

Once the load-shortening curves for elements of the hull cross-section have been obtained, using the method described above, these data can be used to compute the vertical moment-curvature relationship, up to and beyond the collapse moment, for the hull section.

This stage of the analysis is carried out using a simple procedure (4) in which:

(i) vertical curvature of the hull is assumed to occur incrementally: corresponding incremental element strains are calculated on the assumption that plane sections remain plane and that bending occurs about the instantaneous elastic neutral axis of the cross-section; combined vertical and horizontal bending of a hull can be accommodated provided that their relative magnitude and phasing are known and can be represented by incrementing vertical and horizontal curvature;

(ii) element incremental stresses are derived from the incremental strains using the slopes of the stress-strain curves (effective tangent moduli) derived from interframe buckling analysis in the case of longitudinally framed structure (in the case of transversely framed structure use may be made of the load-shortening curves for wide plates as illustrated in Figure 2);

(iii) element stress increments are integrated over the cross-section to obtain bending moment increments, these together with incremental curvatures being summed to provide cumulative values of bending moment M and curvature $\phi$;

Shear forces and shear lag effects in the midships region of a ship's hull are usually negligible: the effects of shear and transverse direct stress can however be accounted for, if significant, by modifying the element load-shortening curves in accordance with data for plates under combined load (15, 20).

HULL-STRENGTH UNDER DYNAMIC LOAD

Whipping of a ship's hull due to slamming (Figure 5) or explosive loading (Figure 6) can cause large additional hull girder bending moments, but, because of their transient nature, these loadings may be less effective in producing plastic collapse than the more slowly varying bending moments due to buoyancy effects. The ultimate hull girder bending analysis method described above is being extended to include dynamic loading in order to investigate how significant whipping stresses are in producing hull failure. This project is still in the development phase but some preliminary results which may be of general interest are reported here.

The elastic response of ships to bow slamming has been studied by many investigators. Extension of strip theory methods to include slamming loads have been reported by Kawakami et al (21), Yamamoto et al (22), Chuang et al (23), Meyerhoff and Schlachter (24) and recently Bishop et al (25) have reported a method of predicting slamming response based on superposition of dry hull modes. A method of analysing the elastic whipping of ships produced by explosive loads has been developed by Hicks (26).

Numerous measurements of slamming stresses in ships at sea have been reported (27 to 31). Figure 7 shows examples of longitudinal deck stresses measured in a frigate during a severe weather sea trial (31). In this case, as in most of the measurements made over the midship region, the whipping was predominantly of the two node mode which has a frequency of 1.7 Hz in this ship (LBP = 110 m). The whipping stress transient is superimposed on that due to wave bending which varies at the wave encounter frequency ($\approx$0.2 Hz in this case).

Fig. 5 Slamming of a Warship in Severe Seas

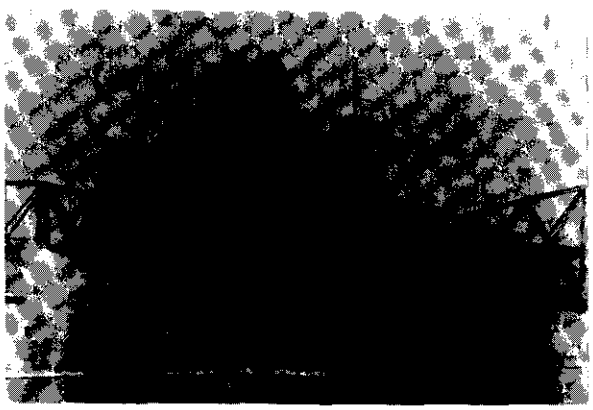

Fig. 6 Whipping of a Warship under Explosive Load

There are two main reasons why higher frequency transients have less effect in producing plastic collapse. Firstly there is a dynamic enhancement of the yield stress at high rates of loading, and secondly the inertia of the structure limits the deformation which can occur within the time of the transient. The first of these is not very significant at the frequencies associated with whipping since the strain rates are too low. A transient to a maximum strain of say 0.2% at 1.7 Hz would give a maximum strain rate of about 0.02 $sec^{-1}$. For medium and high strength steels, Harding (41) has shown that the increase in yield stress is negligible until rates of 10 $sec^{-1}$ and above are reached. Mild steel is more rate sensitive. Campbell (42) shows that the increase in the yield strength is proportional to the log of the strain rate between 0.1 and $10^3$ $sec^{-1}$ (increasing from 264 to 467 MPa over this range) but the increase in yield strength below 0.1 $sec^{-1}$ is small. Since the two node frequency (and hence the strain rate) is approximately inversely proportional to the

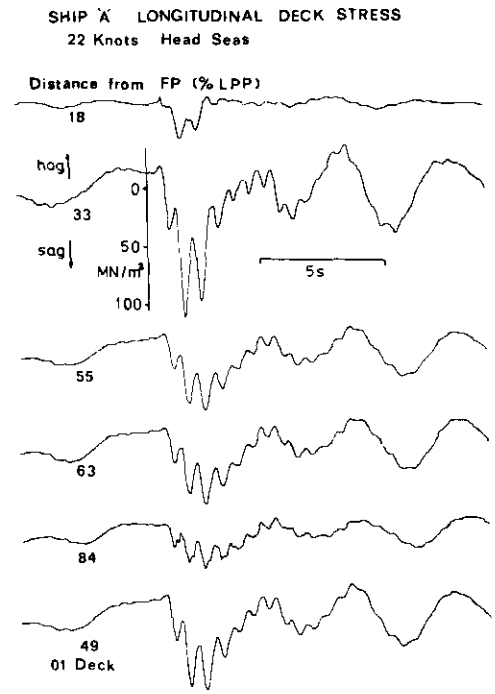


Fig. 7 Measured Slam Induced Whipping Stresses

square root of ship length, dynamic enhancement of yield is only likely to be significant in the higher modes of vibration of short ships.

The main factor to consider in assessing whipping response is therefore the inertia effect. This can be represented by considering the ship as a series of lumped masses connected by elements whose nonlinear bending stiffness is given by the moment/curvature relationships derived from the analysis described above. It can be assumed that the moment/curvature relationship is not affected by inertia effects at whipping frequencies because these frequencies are much lower than the natural vibration frequencies of the stiffened panels included in the analysis.

The hull loading occurring during slamming is mainly over the forward region and can be divided into two types, "bottom impact" which produces high loads but for very short durations (typically $\sim$ 0.1 secs) and "momentum transfer" or "bow flare slamming" which produces lower forces but of much longer duration. Theoretical analysis by Bishop et al (25) suggests that momentum transfer is more important in warships because the resulting bending moments are higher.

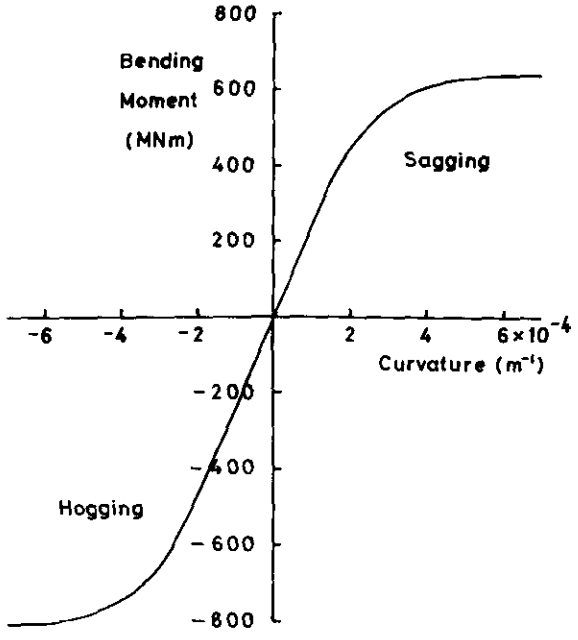


Fig. 8 Destroyer Midships Bending Moment/ Curvature Relationship used in Dynamic Analysis

In a preliminary investigation of the effect of whipping induced plastic collapse, the response of a destroyer to simplified representations of both types of slamming has been analysed. The ship was represented by 21 lumped masses connected by beam elements. The masses included the added water mass associated with the two node whipping mode, although values derived for higher modes were not greatly different. Four elements near the centre, where plastic collapse was expected to occur, were assumed to follow the moment/ curvature relationship shown in Figure 8 which was calculated for the midship section using the method described above. All other beams were assumed to behave elastically.

Figure 9a shows a comparison between the bending moment at midships derived in this way and that derived assuming purely elastic behaviour for a short (0.05 sec) impulse applied near the bow. This was intended to be a simplified representation of "bottom impact" slamming without the complication of the additional more slowly varying loads. In both analyses high frequency modes have been suppressed by numerical damping.

In the absence of a dynamic plasticity calculation failure would have to be assumed to occur at an impulse which produced an elastically calculated moment equal to the maximum value of the moment curvature relationship (640 MNm). The impulse applied for the case shown in Figure 9a was in fact 70% higher

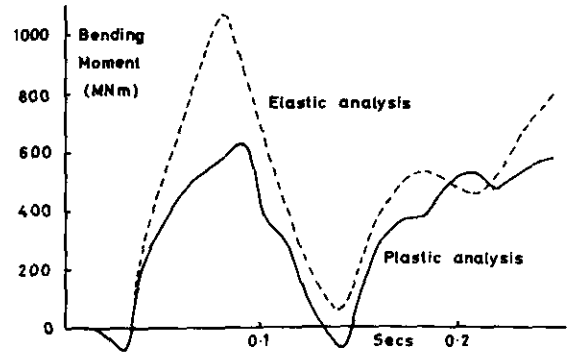


a) Response to 0.05 sec impulse representing bottom impact slamming

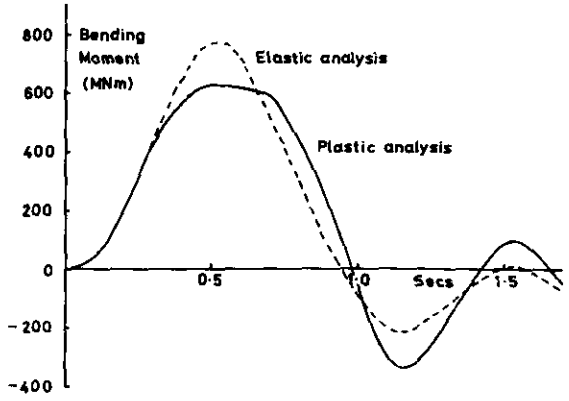


b) Response to 1 sec impulse representing bow flare slamming

Fig. 9 Calculated Bending Moment at Midships Induced by Impulsive Loading

than this value. A similar calculation for an impulse 95% higher became numerically unstable and it must be assumed that the structure would have collapsed under this load. It therefore appears that for short impulses approximating bottom impact slamming, the hull can withstand loads 70-95% higher than the value which produces elastically calculated moments equal to the static collapse value.

As a simplified representation of 'momentum transfer' slamming, calculations have also been carried out for a 1 sec long sinusoidal (half wave) impulse applied to five nodes adjacent to the bow. The resultant bending moment near midships is shown in Figure 9b. The case shown is for an impulse 20% higher than that which gives an elastically

calculated bending moment equal to the static collapse value. A value 30% higher produced collapse. As expected therefore, the dynamic enhancement of failure load is greater for impulses short compared with the natural vibration period of the hull.

These simple representations of the slam loading give an indication of the magnitude of the enhancement of failure load when plasticity effects are taken into account. Further work is now being carried out to analyse more realistic cases where there are superimposed loads due to still water and wave induced bending, and the slam impulse is more accurately represented. Calculations will be based on output from the Bishop & Price analysis method (25) using bottom impact forces calculated from methods derived by Ochi and Motter (32) and Stovovy and Chuang (33).

## ULTIMATE HULL STRENGTH - CORRELATION OF THEORY AND EXPERIMENT

The experimental data available on the ultimate strength of a ship's hull girder when subjected to vertical bending are limited to three important cases. These were the tests on the American destroyers PRESTON and BRUCE (34, 35, 37) in 1930, and those on the British destroyer ALBUERA (36, 37) in 1950, all of which were riveted ships. In the light of this fact the emphasis of the comparisons between theory and experimental data has been placed on welded steel box girder models tested at Imperial College, London and the Technical University, Berlin. These comparisons have been carried out with two main objectives in view:

(a) to validate the theoretical approach for evaluating the ultimate strength of a ship's hull girder subjected to vertical bending;

(b) to investigate the effects of the "hard spots" in the cross-section where buckling is resisted locally by transverse bending stiffness, for example at deck edges and intersections of decks with longitudinal bulkheads or superstructure.

Comparisons of theory and experiment have been carried out for the following cases:

(i) two steel box girders, tested by Dowling et al (38, 39), under conditions of pure bending;

(ii) a steel box girder, tested by Reckling (40), under conditions of pure bending;

(iii) comparison with ultimate longitudinal strength tests carried out on the destroyer ALBUERA.

### (i) Model Tests by Dowling

Dowling (38, 39) has tested a number of steel box girder models subjected to different load conditions. Two of these models, both of which were subjected to pure bending, have been chosen to compare with the theoretical analysis technique.

Experimentally the models chosen both failed by compression flange buckling.

The principal dimensions and properties of the models are shown in Table I(a). The cross-sections were subdivided into stiffened panel elements as shown in the figures in Table I(a). The effective stress-strain curves for these elements were established using the approach outlined previously, residual stress and initial imperfection data used in the analysis are shown in Table II.

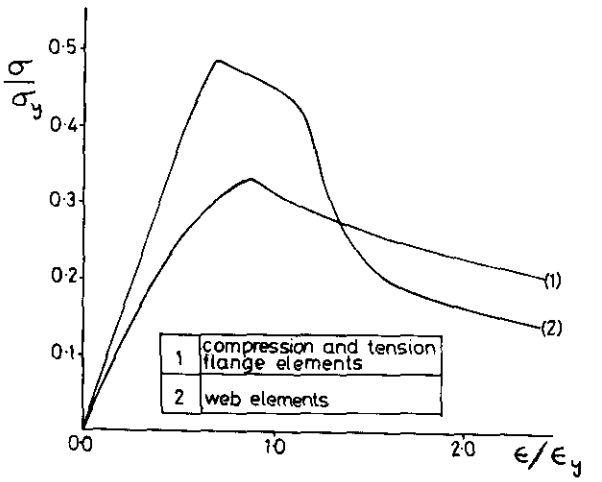


a. Compressive stress/strain curves for stiffened panels

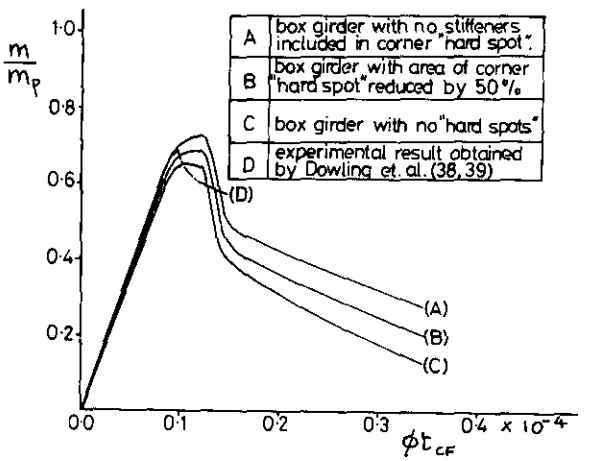


b) Mid-span moment/curvature relationship

Fig. 10 Dowling's Box Girder Model No. 2

TABLE I. PRINCIPAL DIMENSIONS OF MODELS AND PROPERTIES OF MATERIALS

(a) Dowling's Models

| Model No. | Cross section of model dimensions, mm | Component | Nominal size, mm | t*, mm | $\sigma_0$ N/mm² | E N/mm² |
|---|---|---|---|---|---|---|
| 2 | 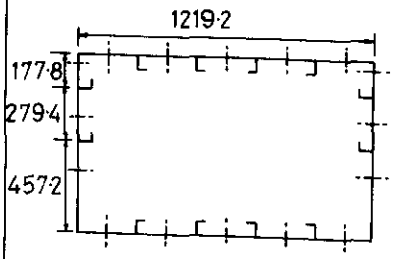 L=787·4 N=5 | CF | 4·76 | 4·88 | 298·0 | 208500 |
| | | TF | 4·76 | 4·88 | 298·0 | 208500 |
| | | W | 3·18 | 3·38 | 211·6 | 216200 |
| | | LS | 50·8x15·9x4·8 L | - | 276·5 | 191500 |
| | | TS | 76·2x50·8x6·4 L | - | 310·4 | 196000 |
| 4 | 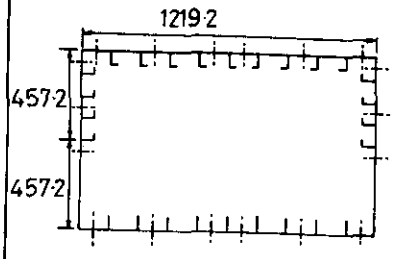 L=787·4 N=5 | CF | 4·76 | 5·03 | 220·9 | 206900 |
| | | TF | 4·76 | 4·95 | 216·2 | 208500 |
| | | W | 4·76 | 4·98 | 281·1 | 216200 |
| | | LS(CF)LS(W) | 50·8x15·9x4·8 L | - | 287·3 | 199200 |
| | | LS(TF) | 50·8x6·4 FLAT | - | 304·3 | 199200 |
| | | TS | 101·6x63·5x6·4 L | - | 304·3 | 206900 |

(b) Reckling's Models

| Model No. | Cross section of model dimensions, mm | Component | Nominal size, mm | t*, mm | $\sigma_0$ N/mm² | E N/mm² |
|---|---|---|---|---|---|---|
| 23 | 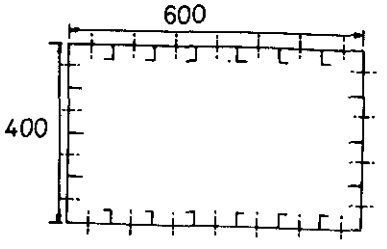 L=500 | CF | 2·5 | - | 246 | 210000 |
| | | TF | 2·5 | - | 246 | 210000 |
| | | W | 2·5 | - | 246 | 210000 |
| | | LS(CF)LS(TF) | 30x20x2·5 L | - | 246 | 210000 |
| | | LS(W) | 30x2·5 FLAT | - | 246 | 210000 |

TF tension flange, LS longitudinal stiffener, LS(CF) longitudinal stiffener on compression flange.
CF compression flange, TS transverse stiffener, LS(TF) longitudinal stiffener on tension flange.
W web, t* measured thickness, LS(W) longitudinal stiffener on web.
N number of bays along span of model
L length between bays

TABLE II. INITIAL IMPERFECTIONS OF TEST MODELS

| Model No. | Maximum stiffener initial deflection * | Maximum plate panel initial deflection | Average longitudinal residual strain † (μ strain) | Average transverse residual strain (μ strain) |
|---|---|---|---|---|
| 2 | +L/2280<br>-L/1450 | b/330 | -250 | - |
| 4 | +L/690<br>-L/510 | - | -600 | - |
| 23 | maximum initial deformation of deck = L/400 | | 0 | - |

* +indicates deflection towards stiffener, -towards plate

† residual strain in plate panels (negative sign indicates compression)

Model No. 2. This model had only four stiffeners on the compression flange; because of this comparatively wide stiffener spacing (50 t) it was assumed that the corner "hard spot" was remote enough from the stiffeners for there to be no stiffening effect on the stiffened panel behaviour. The "hard spot" was therefore assumed to be localised to the corner area only. The compressive effective stress-strain curves for the stiffened panel elements of the cross-section are shown in Figure 10(a), where:

(1) is the effective stress-strain curve for the stiffened plate elements of the compression and tension flanges in compression;

(2) is the effective stress-strain curve for the stiffened plate elements of the webs in compression.

The "hard spots" were assumed to have an elastic-perfectly plastic stress-strain curve corresponding to that of the material in both tension and compression as were the stiffened panel elements in tension. From these stress-strain curves the sagging moment/curvature relationships were computed for the box girder, these are shown in Figure 10(b), where:

(A) represents the moment/curvature relationship for the box girder with the "hard spots" as described above and shown in Table I(a);

(B) same as curve (A) but the areas of the "hard spots" have been reduced by fifty per cent;

(C) same as curve (B) but the "hard spots" on the cross-section have been removed completely;

(D) is the experimental result obtained by Dowling et al.

The bending moment/curvature relationships shown in these and subsequent Figures have been non-dimensionalised by dividing the moment by the fully plastic value (Mp) and multiplying the curvature by the thickness of the compression flange ($t_{CF}$).

It can be seen from Figure 10(b) that these curves bound the experimental values and give a very good prediction of the collapse bending moment for this particular box girder.

These results suggest that for a stiffener spacing of approximately 50 t the "hard spot" has only a localised effect at the corner and does not spread into the stiffened compression flange beyond the first stringer.

Model No. 4. This model was of the same dimensions as Model No. 2 but had many more stiffeners on both the compression and tension flanges than did Model No. 2. It was assumed, because the stiffeners were closely spaced and the end stiffener was very close to the corner of the box girder, that one stiffener would be included in the local "hard spot" at the corner of the box girder. A second analysis which included two stiffeners in the "hard spot" was also carried out for comparison. The compressive effective stress-strain curves for the stiffened panel elements of the cross-section are shown in Figure 11(a), where:

Curve (1) represents the behaviour of both the compression flange and web elements in compression;

Curve (2) represents the behaviour of the tension flange in compression.

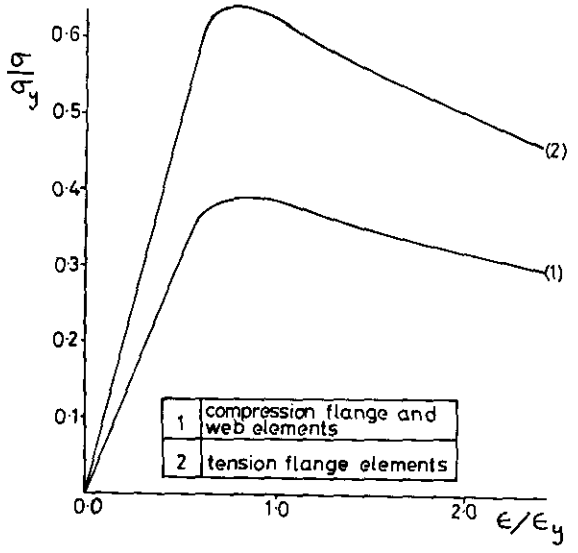


a) Compressive stress/strain curves for stiffened panels

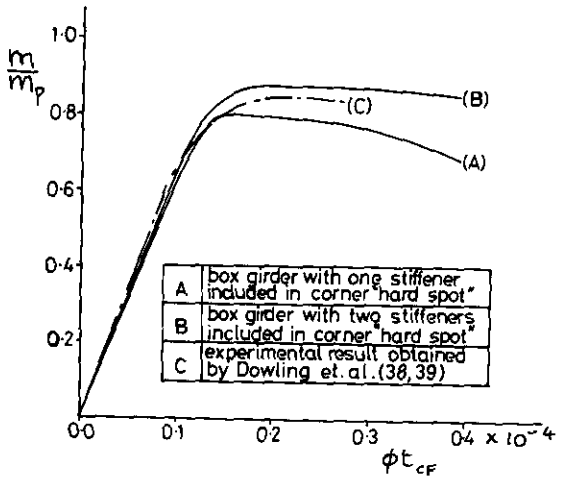


b) Mid-span moment/curvature

Fig. 11 Dowling's Box Girder Model No. 4

The "hard spots" are again assumed to have an elastic-perfectly plastic stress-strain curve in both tension and compression as do the stiffened panel elements which are in tension.

The sagging moment/curvature relationships for the box girder were computed using these stress-strain curves and are shown in Figure 11(b), where:

(A) moment/curvature relationship for box girder where one stiffener is included in local "hard spot" at corner of box girder:

(B) moment/curvature relationship for box girder where a second stiffener is included in the "hard spot";

(C) is the experimental moment/curvature relationship for the box girder obtained by Dowling et al.

It can be seen that the first assumption about the "hard corner" effects, Figure 11(b) Curve (A), yields a collapse load 6% lower than the experimental collapse bending moment for the box girder; the second analysis in which an additional stiffener was included in the corner "hard spot" gives a collapse load 4% higher than the experimental value.

Ignoring other possible inaccuracies in the theoretical model, this result suggests that the stiffening effect of the corner on the compression flange extends between one and two frame spacings into the compression flange for this particular model (stiffener spacing 25 t).

(ii) Model Tests by Reckling

Reckling (40) reported on a series of seven steel box girder tests, all loaded in pure bending, carried out at the Technical University, Berlin. Model No. 23, which had the largest number of stringers and was in this respect most similar to a ship hull, was chosen to compare with the theoretical analysis technique.

Experimentally, Model No. 23 showed a delayed collapse mode where the deck, at first, did not buckle owing to the strengthening effect of the side walls (referred to by Reckling as the "box girder effect") although its plastic buckling strength had been exceeded. Finally, collapse occurred by nearly simultaneous buckling between the stiffeners and of the whole compression flange.

Model No. 23, having principal dimensions and properties shown in Table I(b), was subdivided into stiffened panel elements as shown in the figure of Table I(b). Again, because of the reasonably close stiffener spacing (34 t), the corner "hard spot" was chosen to include one stiffener in its area. The effective stress-strain curves for these elements, being computed using the previously outlined approach with the residual stress and initial imperfection data shown in Table II are shown in Figure 12(a), where:

(1) compressive stress-strain curve for the tension and compression flange elements;

(2) compressive stress-strain curve for the web elements.

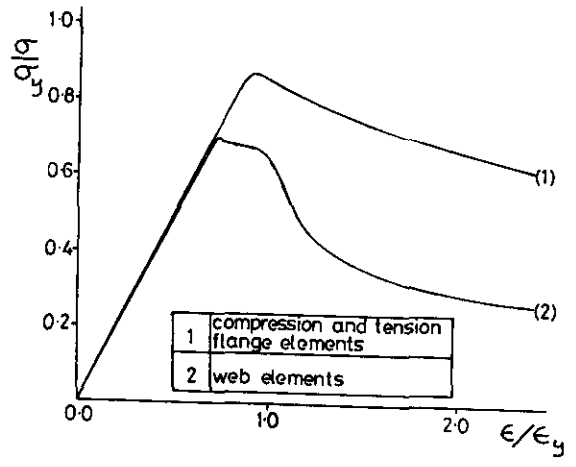


a) Compressive stress/strain curves for stiffened panels

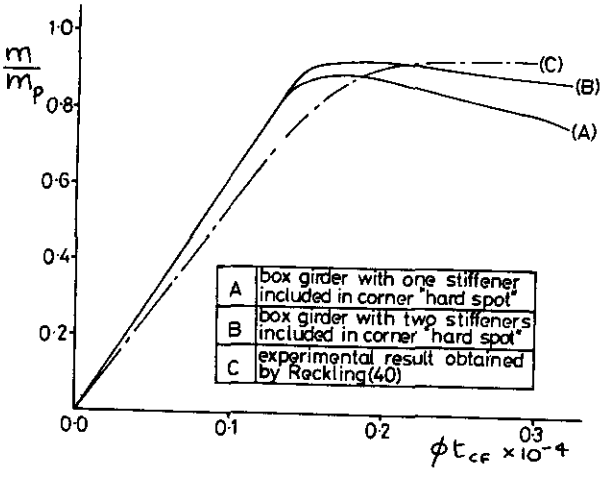


b) Mid-span moment/curvature relationship

Fig. 12 Reckling's Box Girder Model No. 23

The "hard spots" were again assumed to have an elastic-perfectly plastic stress-strain curve in both tension and compression as were the stiffened panel elements in the tension flange.

Using these effective stress-strain curves the sagging bending moment/curvature relationships were computed and are shown in Figure 12(b), where:

(A) corresponds to the box girder with one stiffener included in the "hard spot" at each corner;

(B) represents the case where an additional stiffener is included in the "hard spot";

(C) corresponds to the experimental result obtained by Reckling.

The original assumptions about the "hard corner" effects again produce an estimate of collapse moment 5% lower than the experimental value. Including another stiffener in the area of the hard corner produces almost exactly the experimental collapse moment.

It can also be seen from the moment/curvature graph that the initial stiffness of the box girder observed experimentally is less than that predicted theoretically; possible reasons for this are:

(1) inadequate allowance for initial deformations (because of the lack of detailed information about the plate and stiffener imperfections on the model);

(2) the influence of residual stresses, reported to be zero in the model and ignored in the analysis.

(iii) ALBUERA

Of the three ultimate moment tests carried out on ships, all of which were riveted, it was decided that an attempt would be made to try and predict the collapse moment for the destroyer ALBUERA. This ship was chosen for the following reasons:

(1) The tests on the ALBUERA were originally carried out at NCRE Dunfermline and hence the structural details and experimental data were readily available;

(2) The ALBUERA was longitudinally stiffened and was therefore more like a modern warship, where the American destroyers PRESTON and BRUCE had a transverse framing system.

The midship cross-section of ALBUERA, giving structural details, is shown in Figure 13. The element subdivision is shown in Figure 14. The effective stress-strain curves for the stiffened panel elements were computed in the usual manner and are shown in Figure 15(a); the numbering of the elements in Figure 14 is consistent with the effective stress-strain curves of Figure 15(a). Unnumbered elements correspond to "hard spots" on the cross-section and are assumed to have an elastic-perfectly plastic stress-strain curve in tension and compression. Since the test was carried out with the ship in hogging no compressive stress-strain curve was computed for the deck elements: these were assumed to follow an elastic-perfectly plastic stress-strain curve under tensile load. No information was available on distortion and residual stress levels in the

ALBUERA structure: plate imperfections were therefore assumed rather arbitrarily to be "moderate" (as represented in Figure 1(b)) and stringer deformations were assumed to have the form of uniform curvature of amplitude 0.001 L between transverse frames.

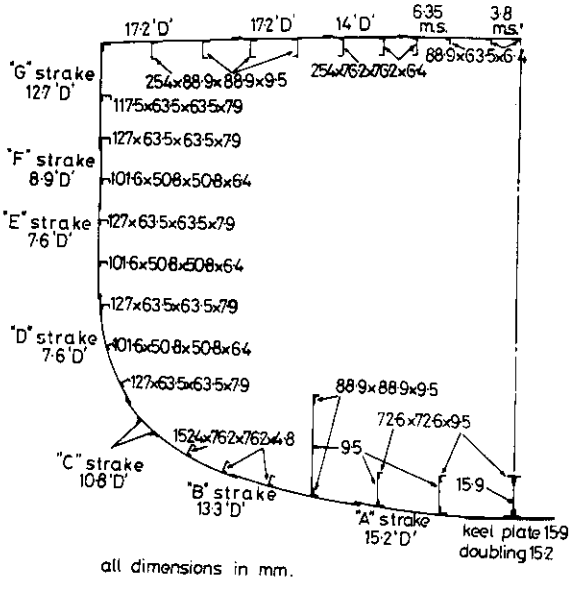


Fig. 13 ALBUERA Midship Section Structural Details

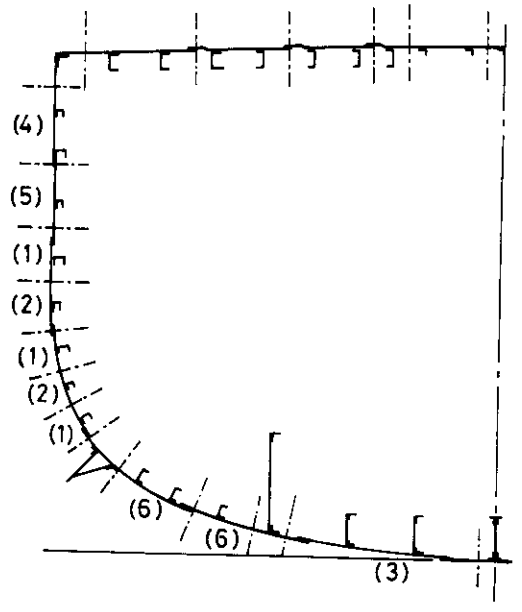


Fig. 14 ALBUERA Midship Section Showing Element Subdivision

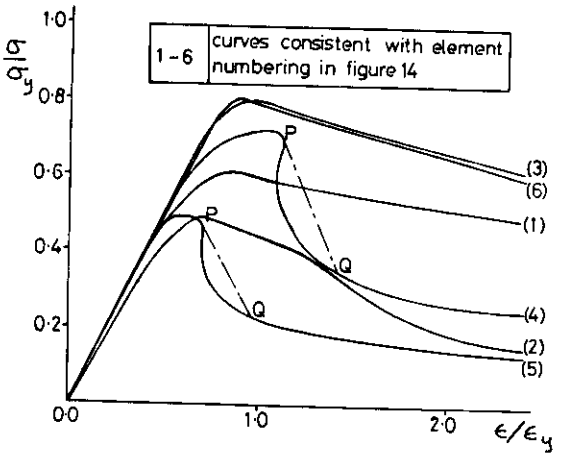


a) Compressive stress/strain curve for stiffened panels

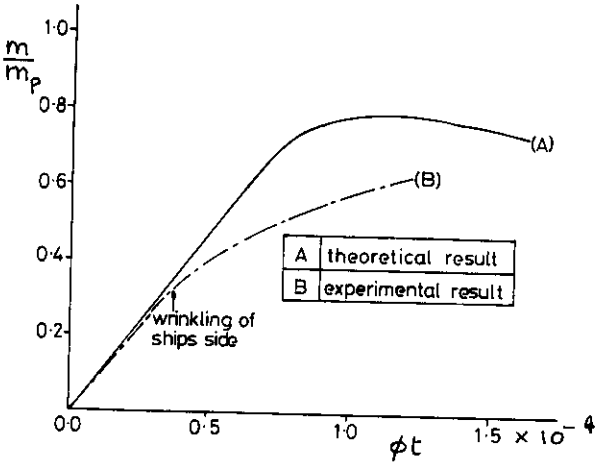


b) Midship moment/curvature relationship

Fig. 15 ALBUERA

In two cases (Curves 4 and 5) unstable post-collapse behaviour was computed; this behaviour will be influenced by the elastic stiffness of the surrounding structure, leading to unloading curves as illustrated by the dotted line in Figure 15(a) where the unloading from points P to Q will occur dynamically. Hence the dotted line path is used to represent post-collapse behaviour instead of the full line curve (which corresponds to the computed, notional, static unloading path).

Using these effective stress-strain curves the hogging moment/curvature relationship for the midship cross-section was computed and is shown in Figure 15(b), where:

(A) represents the hogging bending moment/curvature relationship for the midship cross-section;

(B) indicates the experimental hogging bending moment/curvature relationship.

The theoretically predicted ultimate moment value is 26% in excess of the experimental collapse bending moment. This difference can be attributed to several factors:

(1) No account has been taken in the analysis of rivet slip or the effects of eccentricity of loading due to the overlapping of the plate panels. Neglecting rivet slip in the analysis will have a slight stiffening effect on the elastic part of the theoretical moment/curvature relationship.

(2) The ALBUERA was supported on pairs of blocks similar to those used in the tests on the American destroyer BRUCE. At failure the section which buckled was not the midship section, but frame 72½ which was in fact outside the test section near one of the supports.

(3) The supporting arrangement caused very high shear forces, in conjunction with the high bending moments, at the section where failure finally occurred. In fact, at a reasonably low load level shear buckling of the ship's side occurred thus reducing the stiffness of the section and played an important part in reducing the collapse moment. It is very unlikely that sea loads could develop a vertical shear force and longitudinal bending moment to bring about simultaneous compression and shear buckling as in ALBUERA. No attempt was made to include the effect of these high shear forces in the analysis due to the relatively large amount of work involved to analyse an unrealistic load case. It should be noted at this point that the analysis technique is capable of representing the combination of high shear forces and high bending moments if necessary.

Taking these factors into account the theoretical result is judged to be consistent with the experimental value although the comparison is inevitably rather inconclusive.

## CONCLUSIONS

The problem of evaluating ultimate bending strength of a ship's hull-girder has been discussed and an approximate method of estimating static hull strength, with allowance for local buckling failure of plating and stiffeners has been outlined. Recent numerical studies of the buckling and post-buckling behaviour of plating and stiffened panels have provided data which allow accurate estimates to be made of the stiffness and post-collapse load-carrying capacity of longitudinally or transversely framed deck and shell plating under conditions of biaxial in-plane load, shear and lateral pressure: from the nonlinear stiffness characteristics of elements of a hull section the moment/curvature relationship and hence the collapse strength of a hull-girder may be found by incremental analysis which can account for both vertical and horizontal bending and the presence of shear force and torsion.

The analysis of hull strength under dynamic loads, in particular elasto-plastic hull-girder whipping as may be caused by slamming or underwater explosions, has been discussed and some illustrative results presented. Further work is needed in this area, including particularly development of stable numerical procedures and experimental evaluation of theory.

The proposed method of static hull strength analysis has been correlated with results of experiments on welded steel box-girder models and with collapse tests on the destroyer ALBUERA. Agreement between theory and experiment for small-scale models was satisfactory and gave some guidance on the influence of "hard corners", which undoubtedly have a significant influence on box-girder strength. In the case of ALBUERA, correlation between theory and experiment was less satisfactory: this is attributable mainly to unrealistically high shear forces and premature local failure resulting from the method of load application. It appears, unfortunately, that none of the existing data from hull collapse experiments is capable of providing an accurate check on theory, relating in all cases to riveted and/or transversely framed construction with unknown imperfection levels and being influenced in some cases by unrepresentative, premature local failure. It would clearly be worthwhile to obtain hull collapse data representative of modern, longitudinally framed, welded construction, including careful characterization of imperfections, and it is suggested that energetic efforts should be made by the research community, in collaboration with design and certification authorities, to initiate further hull collapse tests on ships of appropriate type, following completion of service and prior to scrapping.

## REFERENCES


1. J B Caldwell: "Ultimate Longitudinal Strength". Trans RINA, Vol 107, 1965.

2. D Faulkner: contribution to discussion of Reference 1.

3. C V Betts, D M Atwell: "The Ultimate Longitudinal Strength of Ships". Shipbuilding and Shipping Record, p 889, 1965.

4. C S Smith: "Influence of Local Compressive Failure on Ultimate Longitudinal Strength of a Ship's Hull". Proc of Internat Sympos on Practical Design in Shipbuilding (PRADS), Tokyo, October 1977.

5. A E Mansour, A Thayamballi: "Ultimate Strength of a Ship's Hull Girder in Plastic and Bending Modes". Ship Structure Committee Report SSC-299, 1980.

6. D Billingsly: "Hull Girder Response to Extreme Bending Moments". Paper presented at SNAME Spring Meeting, New York, June 1980.

7. D Faulkner: "A Review of Effective Plating for Use in the Analysis of Stiffened Plating in Bending and Compression". Jour Ship Research, Vol 19, No 1, March 1975.

8. K E Moxham: "Theoretical Prediction of the Strength of Welded Steel Plates in Compression". Cambridge Univ Report CUED/C-Struct/TR2, 1971.

9. M A Crisfield: "Full Range Analysis of Steel Plates and Stiffened Plating under Uniaxial Compression". Proc Inst of Civil Engrs, Part 2, Vol 59, December 1975.

10. P A Frieze, P J Dowling, R E Hobbs: "Ultimate Load Behaviour of Plates in Compression". Proc of Internat Conf on Steel Plated Structures, Imperial College, London, July 1976.

11. G H Little: "The Collapse of Rectangular Steel Plates under Uniaxial Compression". The Structural Engineer, Vol 58B, No 3, September 1980.

12. Y Ueda et al: "Ultimate Strength of Square Plates Subjected to Compression". Jour Soc Nav Arch Japan, Vol 137, June 1975 and Vol 140, December 1976.

13. Report of ISSC Committee II.2 on Nonlinear Structural Response, Proc of 7th Internat Ship Structures Congress, Paris, 1979.

14. Report of ISSC Committee III.3 on Fabrication and Service Factors, Proc of Internat Ship Structures Congress, Paris, 1979.

15. P J Dowling et al: "Strength of Ships' Plating under Biaxial Compression". CESLIC Report SP3, Imperial College, London, June 1978.

16. S Valsgard: "Ultimate Capacity of Plates in Transverse Compression". Det Norske Veritas Report No 79-0104, February 1979.

17. C S Smith: "Imperfection Effects and Design Tolerances in Ships and Offshore Structures". Trans Inst Engrs and Shipbuilders in Scotland, February 1981.

18. C S Smith: "Compressive Strength of Welded Steel Ship Grillages". Trans RINA, Vol 117, 1975.

19. R S Dow: "N106C: A Computer Program for Elasto-Plastic, Large Deflection Buckling and Post-Buckling Behaviour of Plane Frames and Stiffened Panels". AMTE(S) R80726, July 1980.

20. J E Harding, R E Hobbs, B G Neal: "The Elasto-Plastic Analysis of Imperfect Square Plates under In-Plane Loading". Proc Inst Civil Engrs, Vol 63, March 1977.

21. M Kawakami, J Michimoto, K Kobashi: "Prediction of Long-Term Whipping Vibration Stress Due to Slamming of Large Full Ship in Rough Seas". International Shipbuilding Progress, Vol 24, No 272, April 1977, p 83.

22. Y Yamamoto, M Fujimo, T Fukaswawa, H Ohtsubo: "Slamming and Whipping of Ships in Rough Seas". EUROMECH Colloquium 122, Paris, September 1979.

23. S Chuang, E A Schroeder, S Wybraniec: "Structural Seaworthiness Digital Computer Program ROSAS". DTNSRDC Report 77-0001, May 1977.

24. W K Meyerhoff, G Schlachter: "An Approach for the Determination of Hull Girder Loads in a Seaway Including Hydrodynamic Impacts". Ocean Engineering, Vol 7, No 2, 1980, p 305.

25. R E D Bishop, W G Price, P K Y Tam: "On the Dynamics of Slamming". Trans RINA 120 (1978) p 259.

26. A N Hicks: "The Theory of Explosion Induced Ship Whipping Motions". NCRE Report R579, March 1972.

27. G Aertssen: "Service Performance and Seakeeping Trials on mv Jordaen". Trans RINA, Vol 108, No 4, 1966.

28. G Aertssen: "Service Performance and Seakeeping Trials on a Large Ore Carrier". Trans RINA, Vol 111, No 2, 1969.

29. G Aertssen, M F van Sluys: "Service Performance and Seakeeping Trials on a Large Containership". Trans RINA, No 4, October 1972.

30. M D Bledsoe, O Bussemaker, W E Cummins: "Seakeeping Trials on Three Dutch Destroyers". SNAME Trans, Vol 68, 1960, p 39.

31. J D Clarke: "Measurement of Hull Stresses in Two Frigates during a Severe Weather Trial". Paper 5, RINA Spring Meeting, 1981.

32. M K Ochi, L E Motter: "Predictions of Slamming Characteristics and Hull Responses for Ship Design". Trans SNAME, 81, 1973, 144-190.

33. A B Stovovy, S L Chuang: "Analytical Determination of Slamming Pressures for High-Speed Vehicles in Waves". Jnl of Ship Research, 20, 1976, 190-198.

34. C O Kell: "Investigation of Structural Characteristics of Destroyers Preston and Bruce, Part 1 - Description". Trans SNAME, Vol 39, 1931.

35. C O Kell: "Investigation of Structural Characteristics of Destroyers Preston and Bruce, Part 2 - Analysis of Data and Results". Trans SNAME, Vol 48, 1940.

36. D W Lang, W G Warren: "Structural Strength Investigations on the Destroyer Albuera". Trans Inst of Naval Arch, Vol 94, 1952, p 243-286.

37. J Vasta: "Lessons Learned from Full Scale Ship Structural Tests". SNAME Trans, Vol 66, 1958, p 165-243.

38. P J Dowling, F M Moolani, P A Frieze: "The Effect of Shear Lag on the Ultimate Strength of Box Girders". Int Cong on Steel Plated Structures, Imperial College, London, July 1976, Paper No 5.

39. P J Dowling, S Chatterjee, P A Frieze, F M Moolani: "Experimental and Predicted Collapse Behaviour of Rectangular Steel Box Girders". Int Conf on Steel Box Girder Bridges, London, 13-14 February 1973.

40. K A Reckling: Preliminary Report on Box Girder Experiments (included in Report of Committee II.2 on Non-linear Structural Response, Proc of 7th Internat Ship Structures Congress, Paris, 1979).

41. J Harding: "Effect of High Strain Rate on the Room Temperature Strength and Ductility of Five Alloy Steels". Jnl of the Iron and Steel Inst, June 1972, p 425.

42. J D Campbell, R H Cooper: "Physical Basis of Yield and Fracture". Inst of Physics and Physical Society, London, 1966.